Journal of Physics: Conference Series **520** (2014) 012006 doi:10.1088/1742-6596/520/1/012006

Graphitized Layer Buried in a Diamond: SAW Generation under Picosecond Optical Excitation

A Klokov, V Tsvetkov, A Sharkov, D Aminev and R Khmelnitskiy

P.N.Lebedev Physical Institute, Moscow, Russia

klokov@sci.lebedev.ru

Abstract. The excitation of SAW was detected on diamond with built-in ion-implanted graphitized layer under its illumination with femtosecond laser pulses. The spectral width of a SAW pulses were in the range of 1.5÷2 GHz. It was found out that the anisotropy of the SAW propagation was practically absent. The increase in the implantation dose from $4 \cdot 10^{15}$ cm^{-2} to $12 \cdot 10^{15}$ cm^{-2} was shown to give rise to a dispersion of SAW propagation.

1. Introduction

Diamond possesses a unique combination of elastic, thermal and electrical properties that makes it an exceptionally attractive material for MEMS as well as for SAW signal processing devices operating in gigahertz range [1]. Formation of various periodical structures is usually required for SAW devices implementation; these periodical structures reflect or simply change the SAW propagation conditions. Such structures can be realized on a basis of ion-implanted graphitized layers build-in the diamond matrix [2]. The information about elastic properties of such layers, e. g., on the sound velocity and attenuation is of high importance. Earlier we have found out that under picosecond optical excitation the bulk coherent phonons are generated by such layers [3]. Depending on the graphitized layer thickness (160-290 nm) and its depth (230-300 nm) the phonons with frequencies in the range of 20 - 120 GHz are generated [4].

This work is devoted to investigations with the help of two-colors picoseconds interferometric method [5] of SAW generation and propagation in structures based on diamond with build-in graphitized layers.

2. Experiment

The buried graphitized layers were created by implanting C^+ ions with the energy of 350 keV into a IIA-type ~300 μm thick natural diamond wafer through a set of masks. Implantation doses are shown in Table 1. The implantation was followed by one-hour vacuum annealing at ~1600°C. The depth of location and thickness of the layers were defined by optical methods similarly to [6] that are shown in Table 1.

The complex refractive index of the layer was n_{Gr}=2.2+j0.88. The reflected light color of those areas with different implantation doses changed from green to dark blue, which was accounted for the interference in optical wavelength range. This allowed us to assume optical perfection of the diamond/graphitized layer interface [7]. The absorption coefficients α of the areas with implanted layers at the wavelength of 400 nm are shown in Table 1.

Table 1. Implantation doses and parameters of buried graphitized layers.

Dose, $\times 10^{15}$ cm^{-2}	Depth, nm	Thickness, nm	α
12	235	283	0.85
10	250	249	0.86
8	265	218	0.92
6	295	160	0.7
4	320	106	0.71

The geometry of the experiment is shown in Figure 1. A femtosecond excitation pulse of the second harmonic of a Ti:sapphire laser was focused on a spot of 3 μm diameter on the surface of the sample. The parameters of the pulse were: τ= 160 fs, λ= 400 нм, E= 0.4 nJ. The minor ($10^{-6} \div 10^{-3}$) changes in the amplitude and in the phase of the first-harmonic pulse of the same laser beam (λ= 800 nm) which was reflected by the sample under investigation, were detected with a Sagnac interferometer [5]. In this interferometer type, the laser pulse is split into two beams, the reference beam and the probe beam. The pulse from the reference beam reaches the specimen before and the pulse from the probe beam after the excitation pulse. The interference of the reference and the probe pulses at the detector generated signals which were proportional to the phase difference δφ= φ(τ)-φ(τ-ΔT), as well as to the sum of relative changes in the modulus δR(τ)/R+δR(τ-ΔT)/R of the reflection coefficient at times τ and τ-ΔT. The sensitivity was ~1 μrad for the phase and ~10^{-6} for the amplitude of the reflection coefficient, respectively; the spatial resolution was ~2 μm, and the time resolution was <1 ps. To study the spatiotemporal distribution of the elastic wave field, the surface of the specimen was scanned with the exciting beam. The experimental setup made it possible to change the time delay τ between the exciting and probing pulses within an interval of 0 to 4 ns.

3. Discussion

In the structures studied, SAW is excited due to the thermoelastic effect after the absorption of the short laser pulse. The experimental data shown below were obtained by registration of the phase changes of the reflection coefficient of the studied layers under propagation of the elastic pulse. We suggest that the variation in the phase of the reflection coefficient occurs mainly due to the displacement of the surface of the specimen and not due to the photoelastic effect.

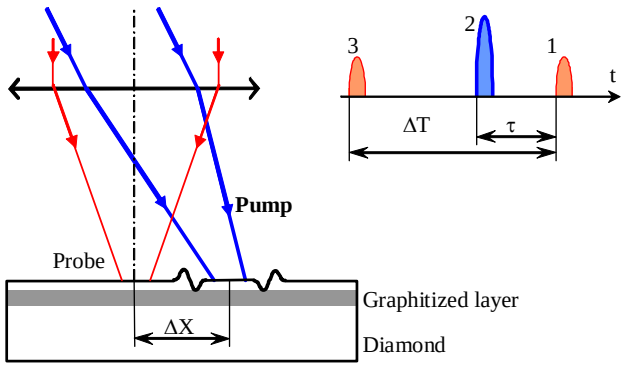

Figure 1. Schematic experimental setup: probe pulse (1) delayed relative to the pump pulse (2). The delay time τ may vary. Δ T is the interval between the arrival of the reference (3) and probe (1) pulses at the sample.

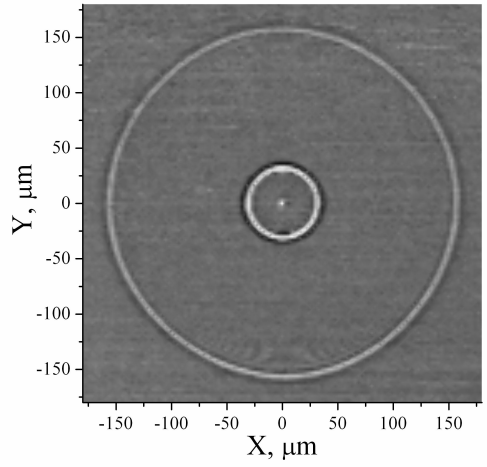

Figure 2. Image of SAW wavefronts. Probe pulse delayed relative to the pump by 3.8 ns

Figure 2 shows the pattern of the SAW field for the area with the implantation dose of $4 \cdot 10^{15}$ cm^{-2}. The probing pulse was delayed by 3.8 ns relative to the exciting pulse. The field distribution appears as concentric rings corresponding to consecutive excitation pulses repeated at 76 MHz frequency. Because of rather low elastic anisotropy of diamond, spatial anisotropy of the SAW propagation was practically absent. A similar pattern of SAW was registered also for area with the implantation dose of $12 \cdot 10^{15}$ cm^{-2}.

To estimate the frequency dispersion, the detection of SAW pulses was performed at various distances between the exciting and the probing spots. Figures 3a and 3b show the shapes of the SAW pulses detected for areas with the doses of $12 \cdot 10^{15}$ cm^{-2} and $4 \cdot 10^{15}$ cm^{-2} respectively.

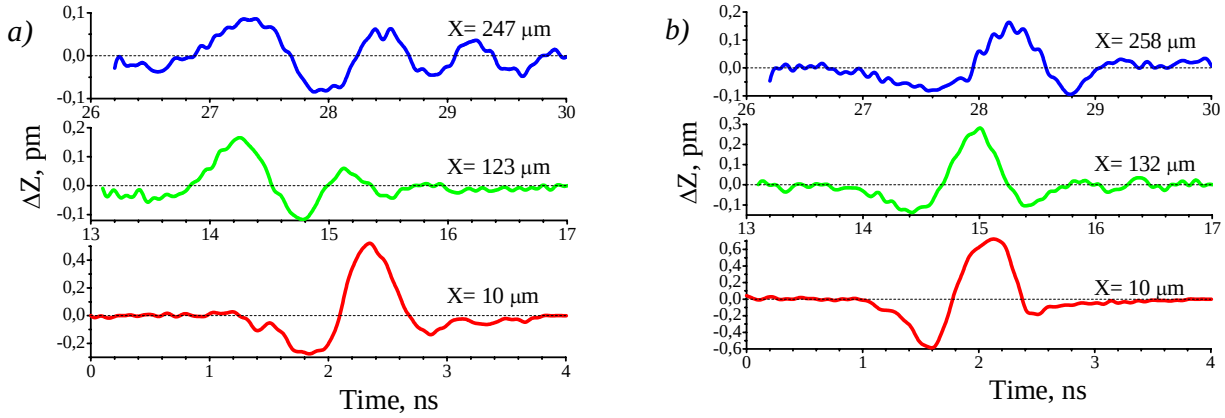

Figure 3. SAW pulses detected *a)* dose $12 \cdot 10^{15}$ cm^{-2}; *b)* dose $4 \cdot 10^{15}$ cm^{-2}. (X - the distance between pump and probe spots)

In both cases, at short distances (~10 μm) between the points of excitation and probing the duration of the pulse was about ~1.2 ns. However, when the distance increased to ~130 μm and further to ~250 μm, the shape of the SAW pulse changed significantly for the area with the higher implantation dose, showing an extension and oscillations. At the same time, for the area with the implantation dose of $4 \cdot 10^{15}$ cm^{-2}, the shape of the pulse showed only a moderate broadening with the increase of the distance.

We performed spectral analysis of the SAW pulses detected at various distances between the exciting and the probing spots. At distances less than 130 μm the spectral width of a SAW pulse was about ~2 GHz, with a maximum at ~700 MHz for all studied areas. For example Figures 4a and 4b shows power spectrum of SAW pulses shown at Figures 3a and 3b.

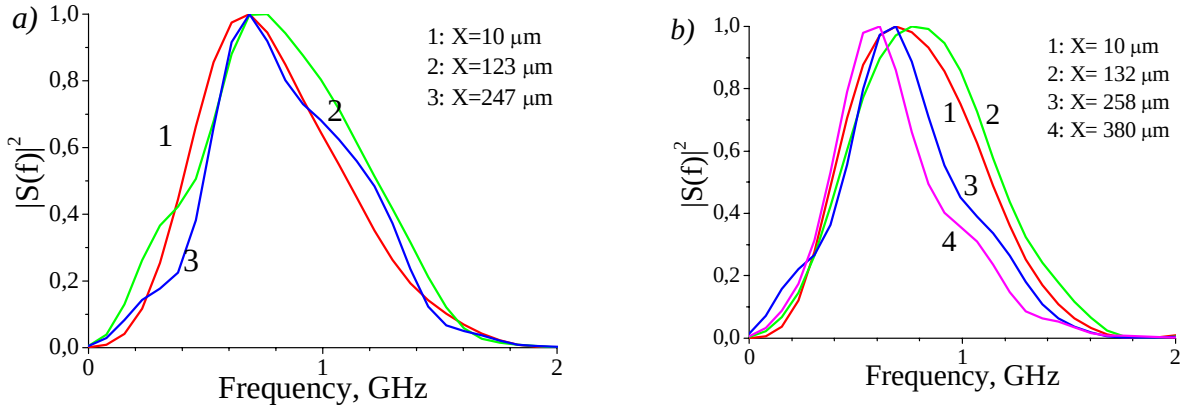

Figure 4. Power spectrum of SAW pulses detected (X - the distance between pump and probe spots). *a)* dose $12 \cdot 10^{15}$ cm^{-2}; *b)* dose $4 \cdot 10^{15}$ cm^{-2}.

With the increase of the distance the pulse spectra for the areas with the implantation doses of $4 \cdot 10^{15}$ cm^{-2} and $6 \cdot 10^{15}$ cm^{-2} narrowed to ~1.5 GHz due to an increased attenuation of the high frequency components in course of propagation of the elastic pulse (Figure 4b). This explains the observed moderate broadening of the SAW pulse for area with dose $4 \cdot 10^{15}$ cm^{-2} at a distance of ~260 μm (Figure 3b). For the areas with the doses of 8, 10 and $12 \cdot 10^{15}$ cm^{-2} the shape of the spectrum was essentially independent of the distance between the exciting and the probing spots (see for example Figure 4a). Therefore, a significant change in the shape of the pulse (Figure 3a) in course of its propagation can be explained by frequency dispersion.

We estimated the phase velocity of SAW propagation over the range of areas of the studied structure similarly to [8]. For the area with a dose of $4 \cdot 10^{15}$ cm^{-2} the velocity did not depend on frequency in a range of up to ~2 GHz and was equal to ~9700 m/s, while for the area with a dose of $12 \cdot 10^{15}$ cm^{-2} the velocity changed from 9900 m/s to 9400 m/s with the increase of frequency by up to 2 GHz. Remarkably, these values are close to the velocity of SAW on intact diamond (~10500 m/s).

In conclusion, we succeeded in detection of SAW excited by subpicosecond optical pulses in diamond with built-in graphitized layer. The absence of anisotropy and considerable difference of acoustical properties from that of diamond makes such layers useful for forming various reflecting, slowing and wave guiding structures.

4. Acknowledgement

We are grateful to V.A.Dravin for diamond implantation, V.P.Martovitsky for X-ray diagnostics and fruitful discussion, and T.I.Galkina for her interest and remarks. This study was supported by the Russian Foundation for Basic Research (projects nos 11-02-01476, 12-02-31865) and by the Russian Academy of Sciences Program of “Basics of Fundamental Research of Nanotechnologies and Nanomaterials”.

References

[1] Krauss A R, Auciello O, Gruen D M, Jayatissa A, Sumant A, Tucek J, Mancini D C, Moldovan N, Erdemir A, Ersoy D, Gardos M N, Busmann H G, Meyer E M and Ding M Q 2001 *Diamond and Related Materials* **10**, 1952-61

[2] Gippius A A, Khmelnitsky R A, Dravin V A and Tkachenko S D *Diamond and Related Materials* 1999 **8** 1631-34

[3] Klokov A, Kochiev M, Sharkov A, Tsvetkov V and Khmelnitskiy R 2011 Graphitized layer buried in a diamond: photothermal properties and hypersound generation under picosecond optical excitation *J. Phys.: Conf. Ser.* **278** 012019

[4] to be published

[5] Tachizaki T, Muroya T, Matsuda O, Sugawara Y, Hurley D H and Wright O B 2006 *Rev. Sci. Instr.* 77, 043713

[6] Khmelnitskiy R A, Dravin V A and Gippius A A 1996 *J. Chem. Vapor Deposition* **5** 121-5

[7] Khomich A V, Khmelnitskiy R A, Dravin V A, Gippius A A, Zavedeev E V and Vlasov I I 2007 *Physics of the Solid State* **49**(9) 1661-65

[8] Neubrand A and Hess P 1992 *Journal of Applied Physic* **71**(1) 227-238